Design of Multidimensional Nonlinear Predictive Controller for 3D Crane

Submitted: 11th November 2023; accepted: 8th February 2024

Maciej Szafrański, Robert Piotrowski

DOI: 10.14313/jamris-2025-013

Abstract:
This paper presents a comprehensive approach to design and implementation of a multidimensional nonlinear control system for a 3D crane. For design purposes, a simulation model of the crane is developed and verified. Proposed are two structures of the control system, which are based on a PID controller and predictive control system. The synthesis process is presented. The designed systems are verified in terms of their effectiveness based on the judgement on the obtained waveforms of controlled variables and integral control indicators. Finally, the two systems are compared with each other, and the conclusions regarding their applicability for this type of system are presented.

Keywords: *3D crane, control systems, mathematical modelling, multidimensional controller, nonlinear MPC controller*

1. Introduction

Throughout history, moving loads of considerable mass has always been a challenge for humans. As a result of industry development, the strength of human hands has been replaced by dedicated industrial machines, such as 3D cranes. Nowadays, they are widely used wherever there is a need to transport enormous or heavy materials from one place to another, especially in production halls.

From the control viewpoint, 3D crane is a dynamic, multidimensional electromechanical system with highly nonlinear dependencies and interactions. Due to the above, designing a proper control system for the crane without an experienced operator to maneuver it is constantly a challenge for engineers. Such a system has to provide safe and precise load transport while controlling load deviations in the specific environment including people and other static or moving devices. Despite these high requirements, modern algorithms can be very effective in controlling cranes.

The designed control system of the crane should be tested before installing it in the device because any possible design errors are likely to cause serious, or even dangerous events, e.g., damaging the crane, or uncontrolled load moving. In order to avoid this, physical models of various types of cranes are commonly used.

The issue is considered in many various studies. The most common approach is to use the structure of the PID controller with gain optimization [1, 2], as it leads to the design of a control system for a linear or linearized crane model, given, for instance, as a number of transfer functions. The second group of strategies are based on fuzzy logic. In [3], the fuzzy logic has been used to describe the 3D crane model and to design a control system for it. In [4, 5], the anti-swing fuzzy controllers have been proposed. The next possibility is to apply model predictive controller (MPC) [6, 7]. These complex algorithms are becoming more and more popular and are a frequent choice, especially in advanced and complex control systems requiring high accuracy and precision. Another alternative solution for controlling the crane is an adaptive controller [8], which can be proposed for uncertain overhead cranes, an LQ controller [9] used in the process control to eliminate unwanted properties of the optimal trajectory, and control algorithms based on visual feedback control of overhead crane [10].

This paper is structured as follows. Section 2 presents the mathematical model of the 3D crane and its verification. In this section, the simulation tests are discussed and equivalent equations for the Z-axis are proposed. Section 3 presents the structure of the proposed control systems and the description of the applied tuning methods. Section 4 provides the analysis of the results of the performed simulation tests, while the concluding remarks are listed in the last section.

2. 3D Crane Description and Modelling

2.1. 3D Crane Description

The analyzed 3D crane is a physical cube-shaped model made by INTECO. It is a representation of actual industrial cranes working in the three axes X, Y, Z of the Cartesian coordinate system to carry various types of loads. In this particular case, a 1 kg load was placed on the lifting rope. The drawing of the model is presented in Fig. 1.

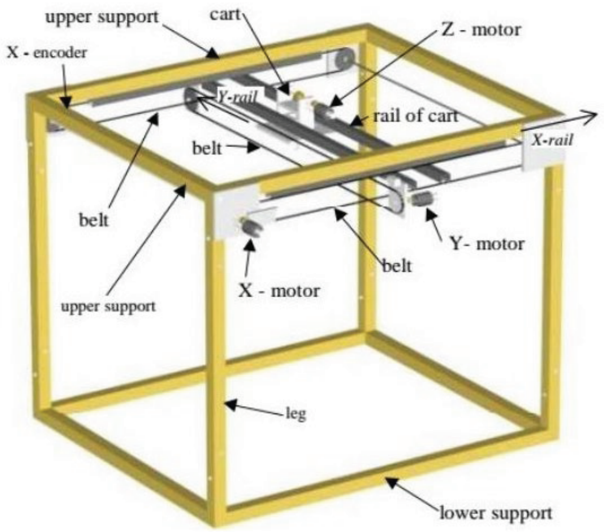

Figure 1. 3D crane

The force used to move the load is generated by three 24 V DC PWM controlled motors. The actual position of the load is measured by 5 high-accuracy incremental encoders in 5 dimensions, which are positions along X-, Y-, and Z-axes, as well as angular deviations between the lifting rope and Y-axis, and between the negative direction on the Z-axis and the projection of the lifting rope onto the XZ plane.

2.2. 3D Crane Modelling

There are several approaches to designing a proper controller for such a multidimensional system. More complex algorithms require very precise information about the behavior of the load and dependencies occurring in the process. This data can be provided as a result of an experiment conducted on the system, or through the theoretical description in the form of mathematical functions and equations. In this study, choosing MPC as one of the proposed controllers defines strictly that the mathematical model is mandatory.

The derivation of the mathematical model of the 3D crane is based on the creation of balance of forces acting along each axis of load displacement, taking into the account the gravity and friction forces, and using Newton's second law for systems with constant mass.

The state space model is considered the most desirable representation. Table 1 presents the state and control variables which have been adopted to receive it. The obtained state space representation describes actual position and velocities of the load with respect to each axis. A number of constant values occur in this representation, which are strictly connected with the physical model. These constant values, collated in Table 2, have been determined by the manufacturer during the development phase.

Table 1. State and control variables of the mathematical model

Variable	Description
x_1	Position X axis [m]
x_2	Linear velocity X axis [m/s]
x_3	Position Y axis [m]
x_4	Linear velocity Y axis [m/s]
x_5	Angular deviation between lifting rope and Y axis [rad]
x_6	Angular velocity for x_5 [rad/s]
x_7	Angular deviation between the negative direction on the Z axis and the projection of the lifting rope onto the XZ plane [rad]
x_8	Angular velocity for x_7 [rad/s]
x_9	Position Z axis [m]
x_{10}	Linear velocity Z axis [m/s]
u_1	PWM control signal for DC motor in X axis [-]
u_2	PWM control signal for DC motor in Y axis [-]
u_3	PWM control signal for DC motor in Z axis [-]

Table 2. Constant parameters of the 3D crane model

Parameter	Variable	Value
Load weight	m_c	1 kg
Boogie weight	m_w	1.155 kg
Bus weight	m_s	2.2 kg
Friction force axis X	T_x	100 N
Friction force axis Y	T_y	82 N
Friction force axis Z	T_z	75 N

The final model is highly nonlinear and complex. There are many correlations between state variables:

$$\frac{dx_1(t)}{dt} = x_2(t) \tag{1}$$

$$\frac{dx_2(t)}{dt} = U_{n1}(t) + w + m_{i1}c_5U_{n3}(t) - m_{i1}c_5z \tag{2}$$

$$\frac{dx_3(t)}{dt} = x_4(t) \tag{3}$$

$$\frac{dx_4(t)}{dt} = U_{n2}(t) - r + m_{i2}s_5s_7U_{n3}(t) - m_{i2}s_5s_7z \tag{4}$$

$$\frac{dx_5(t)}{dt} = x_6(t) \tag{5}$$

$$\begin{aligned}\frac{dx_6(t)}{dt} = \frac{1}{x_9(t)}(&ws_5 + U_{n1}(t)s_5 \\ &+ s_5c_5x_9(t)(x_8(t))^2 - c_5U_{n2}(t)s_7 \\ &+ gc_5{}^2 - c_5m_{i2}s_5s_7{}^2U_{n3}(t) \\ &+ c_5m_{i2}s_5s_7{}^2z + c_5rs_7 + c_5m_{i1}s_5U_{n3}(t) \\ &- c_5m_{i1}zs_5 - 2x_{10}(t)x_6(t))\end{aligned} \tag{6}$$

$$\left\{\frac{dx_7(t)}{dt} = x_8(t)\right. \tag{7}$$

$$\frac{dx_8(t)}{dt} = \frac{1}{x_9(t)\,s_5}\big(-c_7 U_{n2}(t) + g s_7 + 2x_6(t)\,x_8(t)\,x_9(t)\,c_5 + c_7 m_{i2} s_5 s_7 U_{n3}(t) - c_7 m_{i2} s_5 s_7 z + 2x_8(t)\,x_{10}(t)\,s_5 - c_7 r\big) \tag{8}$$

$$\frac{dx_9(t)}{dt} = x_{10}(t) \tag{9}$$

$$\frac{dx_{10}(t)}{dt} = -c_5 w - c_5 U_{n1}(t) + x_9(t) {s_5}^2 x_8(t)^2 - s_5 s_7 U_{n3}(t) + g s_5 c_7 - m_{i2} {s_5}^2 {s_7}^2 U_{n3}(t) + m_{i2} {s_5}^2 {s_7}^2 z + r s_5 s_7 - m_{i1} U_{n3}(t) + m_{i1} U_{n3}(t)\, {s_5}^2 + m_{i1} z - m_{i1} z {s_5}^2 + x_9(t)\, x_6(t)^2 - U_{n3}(t) + z \tag{10}$$

where:

$$n = -T_3 x_{10}(t) - T_{sz}\, sign(x_{10}(t)) \tag{11}$$

$$r = T_2 x_4(t) + T_{sx}\, sign(x_4(t)) \tag{12}$$

$$w = -T_1 x_2(t) - T_{sy}\, sign(x_2(t)) \tag{13}$$

$$c_5 = \cos(x_5(t)) \tag{14}$$

$$s_7 = \sin(x_7(t)) \tag{15}$$

$$c_7 = \cos(x_7(t)) \tag{16}$$

$$U_{n1}(t) = \frac{40\, u_1(t)}{m_w} \tag{17}$$

$$U_{n2}(t) = \frac{34\, u_2(t)}{m_w + m_c} \tag{18}$$

$$U_{n3}(t) = \frac{-g\, u_3(t)}{m_c} \tag{19}$$

$$m_{i1} = \frac{m_c}{m_w} \tag{20}$$

$$m_{i2} = \frac{m_c}{m_w + m_s} \tag{21}$$

$$T_1 = \frac{T_y}{m_w} \tag{22}$$

$$T_2 = \frac{T_x}{m_w + m_s} \tag{23}$$

$$T_3 = \frac{T_z}{m_c} \tag{24}$$

$$T_{sx} = \frac{5}{m_w + m_s} \tag{25}$$

$$T_{sy} = \frac{7.5}{m_w} \tag{26}$$

$$T_{sz} = \frac{10}{m_c} \tag{27}$$

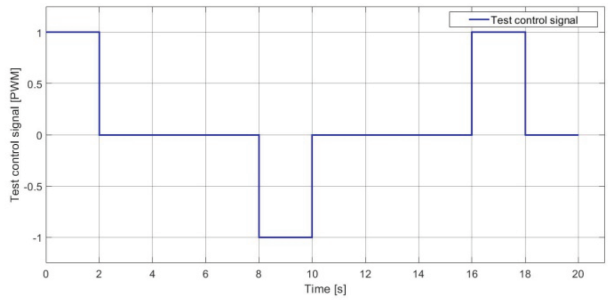

Figure 2. Test control signal

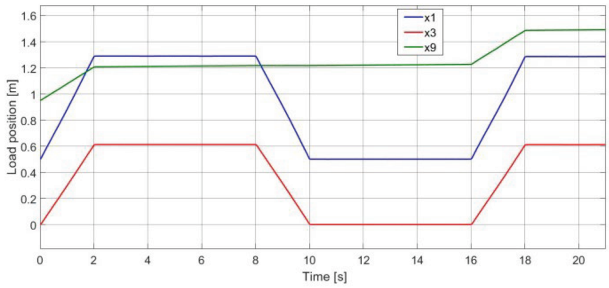

Figure 3. Position of load

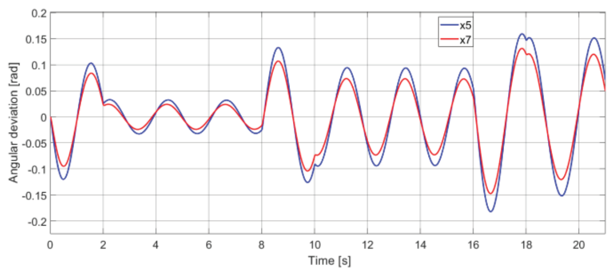

Figure 4. Angular deviation of load

2.3. Simulation Tests and Model Verification

The state space model has been implemented in Matlab environment. Before starting the synthesis of the control system, the simulation tests were performed. The test signal was designed as shown in Fig. 2 and set for all control signals simultaneously to verify the behavior of the 3D crane. The results are shown in Figs. 3–4.

The model reacts correctly to a positive and negative force acting along the X- and Y-axes – the position of the crane along these axes returns to its original values (see Fig. 3). However, the tests have revealed that the model does not work properly along the Z-axis. As shown in Fig. 2, the negative control signal was applied between second 8 and 10 of the simulation process. The load position values slightly increased, but this seems to be the effect of other inputs and current deviation of the load, and not of the input applied to the device controlling the Z-axis.

The model reacts correctly to a positive and negative force acting along the X- and Y-axes – the position of the crane along these axes returns to its original values (see Fig. 3).

However, the tests have revealed that the model does not work properly along the Z-axis. As shown in Fig. 2, the negative control signal was applied between second 8 and 10 of the simulation process. The load position values slightly increased, but this seems to be the effect of other inputs and current deviation of the load, and not of the input applied to the device controlling the Z-axis.

Whenever the control signal is changed to a non-zero value, the deviation increases (see Fig. 4). When it is equal to zero, the system is observed to be self-stabilizing. The reaction of the system is noticeable, as expected, the rope with the load deflects more when the momentum of DC motors is applied to the crane.

This behavior may be caused by erroneous derivation of the equations composing the mathematical model. In this case, the synthesis of the control system in which the controller requires full knowledge of the mathematical model in the state-space form may be burdened with a large error. Moreover, the simulation model working in this way excludes the validity of creating a control system.

Because of the above conclusion, the part of the model connected with the Z-axis had to be redesigned. A solution was found in the 3D crane documentation attached to the device. The manufacturer performed relevant tests and derived the linearized model of the Z-axis in the form of a transfer function. With the use of a simple mathematical apparatus, the transition between the transfer function and the state space model for the Z-axis was determined. The new equation describing the velocity along the Z-axis replaced Eq. (10) in the model, thus creating the final mathematical representation of the 3D crane:

$$\frac{dx_{10}(t)}{dt} = \begin{cases} 5.2233\,u_z\,(t) \\ -50.6816 x_{z1}(t) \quad dla\,u_z \geq 0 \\ 7.0826\,u_z\,(t) \\ -77.2379 x_{z1}(t) \quad dla\,u_z < 0 \end{cases} \tag{28}$$

3. Design of Control Algorithms

Designing a control system for various types of 3D cranes is a common problem in industrial automation. Physical models of cranes implemented for scientific purposes are also popular. Therefore, many designers are facing the issue of selecting the controller and the structure of the control system for the crane. The needs, requirements, and possibilities have to be defined in this case. It is worth taking under consideration aspects such as the control method, the repeatability of movements, financial possibilities, and physical limitations, for instance, in the production hall.

The structure of the system used in this work allows the use of virtually any control method. The requirements on the control system come down to maintaining and tracking the set trajectory of the load while minimizing angular deviations of the load. Two different control systems have been proposed for the 3D crane, which are based on the PID controller, and nonlinear MPC (NMPC).

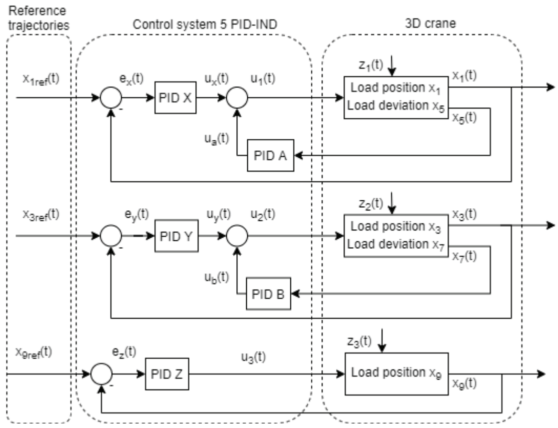

Figure 5. The structure of 3D crane control system with 5 PID controllers

3.1. PID Controller

The PID controller is very commonly used in the industry. It is a classic controller based on the measurement of the system or model output. The system with such a controller is primarily simple to implement. Another huge advantage of the PID controller is that it does not require knowledge of the system's model, which allows the control system designer to avoid the modelling phase [11].

The experiment has been selected as the tuning method. It is a technique based on tuning the controllers' gain values while observing and analyzing the output and control signals. The effectiveness of this method is strongly related to the skills of the control system designer. To be fully effective, the method requires experience and knowledge about the controller's behavior, and about the influence of each gain to the output. Using some control quality indicators, e.g., control error, or overshoot, is highly recommended during the whole tuning process. When using this type of approach directly on the system, the designer has to be careful because improper selection of settings may result in the loss of system stability.

The first proposed control system consists of 5 PID-IND controllers (see Fig. 5) where three of them are responsible for controlling the load in 3D and the remaining two compensate for the load deviation.

where x_{1ref}, x_{3ref}, x_{9ref} are reference position signals in X-, Y- and Z-axis directions, e_x, e_y, e_z are control errors, u_x, u_a, u_1, u_y, u_b, u_3 are control signals, z_1, z_2, z_3 describe disturbances which affect the system, and e_x, e_y, e_z) and x_1, x_3, x_5, x_7, x_9 are state variables.

In order to provide error control for both load position and deviation, a 2 PID cascade controller has been used. In that way the controller can generate the counter phase control signal working against the deviation, while balancing near the setpoint position of the crane load. For the Z-axis, a simple closed loop structure has been proposed.

From the control viewpoint, the accuracy of reaching the set position with small deviation is more important than the time of reaching this position.

For this particular reason, when tuning PID_x, PID_y, and PID_z, attention was paid for overshoot not to exceed 10% of the setpoint value.

3.2. Nonlinear MPC

Predictive control is an advanced control method used in situations where there is a need for high accuracy, predictability of control, and safety maintenance. The basic requirement for making the implementation of MPC possible is the knowledge of the mathematical model of the system. Unlike classic control systems, the MPC system is not based solely on changes in the output signals from the facility, as it generates control signals by solving the optimization problem based on the knowledge of the mathematical model, the controls in previous moments of time, and the measurements of output values.

Firstly, the decision variables have to be defined. In this work, these are all available state variables describing the position of the load x_1, x_3, x_9, the angular deviation x_5 and x_7, and the linear and angular velocities x_2, x_4, x_6, x_8, x_{10} in the system.

Next, the objective function was defined as the weighted sum of deviations of the controlled states from their reference trajectory and the control values representing the cost of their incurring. Its formula is given as:

$$\min(x) = min\left\{\sum_{i=1}^{5} w_i \sum_{p=1}^{H_c} x_{ref}(k+p|k) - x(k+p|k)\right]^2 + \sum_{j=1}^{3} w_j \sum_{p=1}^{H_c} \mathrm{u(k+p|k)} \tag{29}$$

where J is the current value of the objective function, k is the discrete time sample, (w_i, w_j) are the weight values, x_{ref} (k + p|k) is a reference value, $x\,(k{+}p|k)$ is the predicted value of state variable, and u(k + p|k) is the calculated control signal.

Finally, the constraints for the optimization task have been set as:

$$u_1^{min} = u_2^{min} = u_3^{min} = -0.3 \tag{30a}$$

$$u_1^{max} = u_2^{max} = u_3^{max} = 0.3 \tag{30b}$$

Fig. 6 presents the idea of the predictive controller algorithm.

where x_{ref} is the matrix of reference position signals in X-, Y- and Z-axis directions, e* is the matrix of predictive control errors, u* is the control signal generated by the optimizer during the optimization process, x* is the matrix of calculated state variables, u is the matrix of generated control signals, and x is the matrix of states variables

The optimizer retrieves the information about the given trajectories and current values of decision variables. Then it solves the optimization problem for the defined objective function, taking into account the assumed constraints.

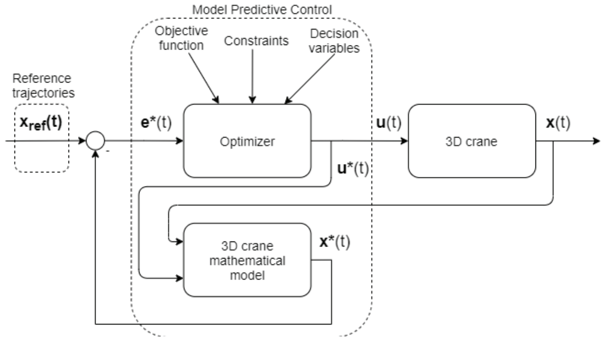

Figure 6. The structure of 3D crane predictive control system

To achieve this goal, it uses the existing mathematical model of the crane, applying future controls to the system and calculating its predicted outputs. After finding the best solution, the first calculated controls are set at the controller output. Then the whole procedure starts again, using new system state values and setpoints [12].

4. Control Results

4.1. Simulation Conditions

The implemented control systems have been tested. To allow for the comparison of different control systems, certain quality criteria had to be adopted. For the control systems, these criteria can be defined in many different ways, starting from the shape of the output signals, through overshoots, and ending with purely numerical indicators.

This article does not examine the effect of mass values on the performance of the control system. A constant mass was assumed.

For the purposes of this work, two integral indices: Integral Square Error (ISE) and Integral Absolute Error (IAE) have been selected to assess the quality of the designed control systems. The mathematical description of these criteria is given by dependencies (31a) and (31b).

$$ISE = \int_0^\infty (\mathrm{e(t)})^2 \mathrm{dt} \tag{31a}$$

$$IAE = \int_0^\infty |\mathrm{e\,(t)}|\,\mathrm{dt} \tag{31b}$$

Moreover, the initial conditions for the position of the load were defined: $x_{1p} = x_{3p} = 0.3$, $x_{9p} = 0.95$, where x_{ip} is the initial condition for the i-th state variable, i=1,...,10. ll other initial values of state variables in the 3D crane model have been assigned with zero values.

4.2. Control Results for PID Controller

Tuning PID controllers started with the controllers responsible for the load position along X-, Y-, and Z-axes. Only after that, the settings for the load deviation controllers were selected. For the purposes of the simulation study, three different sets of PID controllers were proposed (see Table 3).

The first set, presented in Table 3, was introduced to verify whether the system can handle controlling without the feedback from the deviation PID controllers.

Although the system is most accurate for the load position along the Y-axis, the entire control system, according to Tables 4 and 5, is the worst out of all the three proposed. This leads to the conclusion that load deviation has to be controlled in the system to increase precision.

In the second variant, PID A and PID B were tuned. The position indicators in the directions of X-, Y-, and Z-axes have values similar to the first option, however, the values of the indicators for deviations are undoubtedly better.

In the last variant, the values of proportional gains for PID alpha and PID beta controllers were increased. In addition, the derivative gain was assigned. Thanks to its positive influence on the transient states, the system is characterized by the best total IAE and ISE indicators among all proposed variants of PID controllers.

In summary, for the PID structure control system, the load deviations have to be taken into account, as the deviation feedback provides leads for the system to undulate the load position, and thus, slowly eliminate the load swing effect.

4.3. Control Results for Nonlinear MPC

During the simulation tests, different combinations of individual weight values were checked in terms of their influence on the behavior of the control system (see Table 6). As a result, three variants illustrating the shaping of the weight values and their impact on the operation of the controller were proposed. During the test, the control horizon was given the constant value: $H_c = 4$.

The analysis of Tables 7 and 8 shows that small weight values responsible for load deviation (w_4, w_5) improve the indicator values for both x_5 and x_7. However, if this value is too high, as in the last variant proposed in Table 6, the control quality for the position along the Y-axis is poor according to IAE. In addition, w_3 has to be greater than w_1 and w_2, because if they are equal, the controlling along the Z-axis is much worse than when a larger value is set for this weight. The best values of ISE and IAE were obtained in the third variant.

The next tests concerned the determination of the control horizon (see Tables 9 and 10). They were carried out for three different values of the control horizon, using the weights of the best variant from Table 6.

The control system is the least precise for $H_c = 2$, in terms of the realized load position along each axis. Moreover, it does not have the ability to extinguish oscillations that occur. For $H_c = 4$, the system very precisely controls the position of the load. The deviation α is much better damped than for $H_c = 2$. As for the deviation β, slight decay of oscillations can be observed.

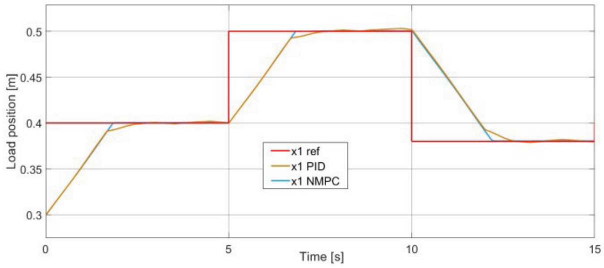

Figure 7. Obtained waveforms of tracking reference trajectory x_1 for both designed control systems

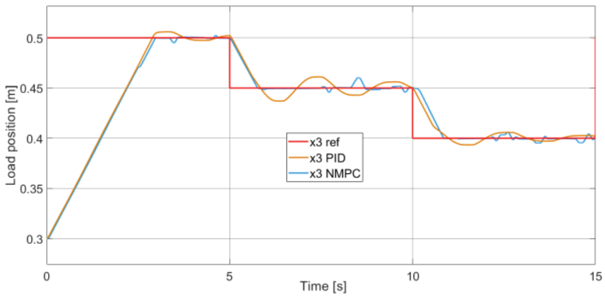

Figure 8. Obtained waveforms of tracking reference trajectory x_3 for both designed control systems

Finally, when $H_c = 6$, the system is slightly less accurate in controlling the position axes than for $H_c = 4$. However, some favorable difference in deviation control is noticeable in this case.

Greater values of the control horizon were also checked during the test simulation, however the improvement of system quality turned out insignificant compared to the extension of the calculation and simulation time of the control system.

4.4. Comparative Analysis

The final step of the performed tests was the comparison between the best received PID control system, presented as variant 3 in Table 3, and the NMPC control system, presented as variant 3 in Table 6 with $H_c = 6$.

Looking at the total values of the indicators, shown in Tables 4, 5, 9, and 10, a clear difference can be observed between the designed control systems in favor of the PID structure. However, individual values of the controlled quantities for load position x_1, x_3, x_9, and load deviation x_5 are better for the predictive control system. The only control state for which the individual indicators are better for the PID control system is the load deviation x_7.

The next part of the comparison concerned the obtained waveforms. Figs. 7–9 show the load position results obtained for both designed control systems.

The presented waveforms indicate that the two designed control systems work properly. They follow the given reference trajectory of load position along all three axes. They also counteract excessive overshoot as they smoothly get to the set position.

Table 3. Proposed gains of PID controllers

No.	PID X	PID Y	PID Z	PID A	PID B
1	$kp = 33$ $ki = 0.4$ $kd = 0$	$kp = 41$ $ki = 0.1$ $kd = 0$	$kp = 50$ $ki = 0.2$ $kd = 0$	$kp = 0$ $ki = 0$ $kd = 0$	$kp = 0$ $ki = 0$ $kd = 0$
2	$kp = 33$ $ki = 0.4$ $kd = 0$	$kp = 41$ $ki = 0.1$ $kd = 0$	$kp = 50$ $ki = 0.2$ $kd = 0$	$kp = 10$ $ki = 0.2$ $kd = 0$	$kp = 10$ $ki = 0.3$ $kd = 0$
3	$kp = 33$ $ki = 0.4$ $kd = 0.2$	$kp = 41$ $ki = 0.1$ $kd = 0,32$	$kp = 50$ $ki = 0.2$ $kd = 0.1$	$kp = 15$ $ki = 0.2$ $kd = 0.05$	$kp = 17$ $ki = 0.3$ $kd = 0.2$

Table 4. IAE for PID controllers

No.	x_1	x_3	x_9	x_5	x_7	Sum
1	0.3451	0.345	0.253	0.1945	0.3759	1.513
2	0.342	0.3646	0.253	0.1164	0.248	1.324
3	0.3413	0.3788	0.253	0.1077	0.2022	1.283

Table 5. ISE for PID controllers

No.	x_1	x_3	x_9	x_5	x_7	Sum
1	0.02403	0.04063	0.01387	0.003578	0.01483	0.09693
2	0,02398	0,04076	0,01387	0,00133	0,005404	0,08534
3	0,02402	0,04096	0,01387	0,001256	0,003864	0,08397

Table 6. Weight values for NMPC controller

No.	w_1	w_2	w_3	w_4	w_5	w_6	w_7	w_8
1	1000	1000	1000	0	0	0.001	0.001	0.001
2	1000	1000	3000	0.03	0.03	0.01	0.01	0.01
3	1000	1000	3000	0.03	0.03	0.0005	0.0005	0.0005
4	1000	1000	3000	1	1	0.001	0.001	0.001

Table 7. IAE for NMPC controller – tuning the weight values with constant H_p

No.	x_1	x_3	x_9	x_5	x_7	Sum
1	0.3249	0.35	0.3904	0.0874	0.4617	1.614
2	0.3742	0.4531	0.3978	0.1022	0.4505	1.778
3	0.3243	0.3507	0.2591	0.08956	0.4705	1.494
4	0.3227	0.5025	0.2551	0.08911	0.5194	1.689

Table 8. ISE for NMPC controller – tuning the weight values with constant H_p

No.	x_1	x_3	x_9	x_5	x_7	Sum
1	0.02347	0.04116	0.02141	0.0008966	0.02083	0.1078
2	0.02349	0.04272	0.01805	0.001013	0.01973	0.105
3	0.02347	0.04171	0.01386	0.00092	0.02129	0.1013
4	0.02353	0.0463	0.01375	0.0008992	0.02578	0.1103

Table 9. IAE for NMPC controller – tuning the control horizon H_p

H_c.	x_1	x_3	x_9	x_5	x_7	Sum
H_c=2	0.3335	0.3589	0.3007	0.09413	0.4805	1.568
H_c=4	0.3243	0.3507	0.2591	0.08956	0.4705	1.494
H_c=6	0.326	0.3552	0.2607	0.08828	0.4496	1.48

Comparing the operation of both systems, for x_1 the NMPC control system is slightly more precise than the PID control system as it gets to the desired position faster.

For x_3, the PID control system gently falls into slow oscillations in order to control the load deviation, while the NMPC does less frequent and more dynamic counteractions - the system returns to the desired

Table 10. ISE for NMPC controller – tuning the control horizon H_p

H_c	x_1	x_3	x_9	x_5	x_7	Sum
H_c=2	0.02313	0.04175	0.01481	0.0009334	0.02222	0.1028
H_c=4	0.02347	0.04171	0.01386	0.00092	0.02129	0.1013
H_c=6	0.0236	0.04202	0.01357	0.0009144	0.01989	0.09999

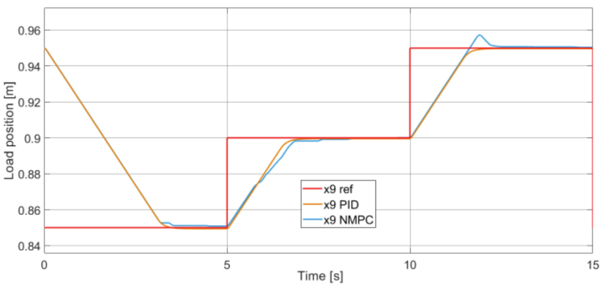

Figure 9. Obtained waveforms of tracking reference trajectory x_9 for both designed control systems

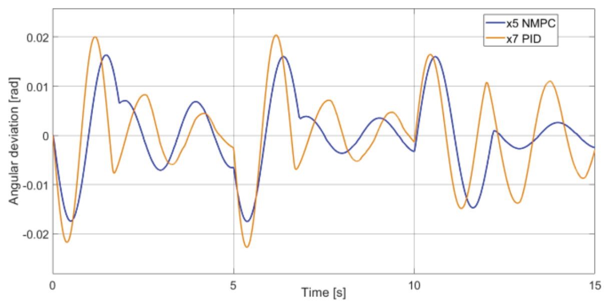

Figure 10. Obtained waveforms of x_5 control for both designed control systems

position faster. For x_9, the systems work in a quite similar way until the last set values are reached. Then the NMPC controller generates an overshoot and returns to tracking the set value together with reaching the x_1 reference position, while the PID structure reaches the position without such actions.

The overshoot generated by the NMPC controller for x_9 allows it to counteract effectively the increase of x_5 deviation, thus reducing it to a negligible value, as shown in Fig. 10. This system turns out to perform better in controlling x_5 than the PID control system.

For x_7 deviation, NMPC performs much worse than the PID control system, as can be seen in Fig. 11. It can be stated that the NMPC tries to counteract this deviation only for the last set values. At the same time, the PID control system tries to control x_7 throughout the entire duration of the control.

Summing up, the NMPC system is certainly a solution which can be considered for 3D crane control. The error related to the adjustment of x_7 can be related to the error in the original simulation model. Therefore, the obtained system may not work properly as some information and dependencies are lost. Nevertheless, in the remaining cases, the control quality is satisfying. However, it should be noted that the control horizon plays an important role in this case.

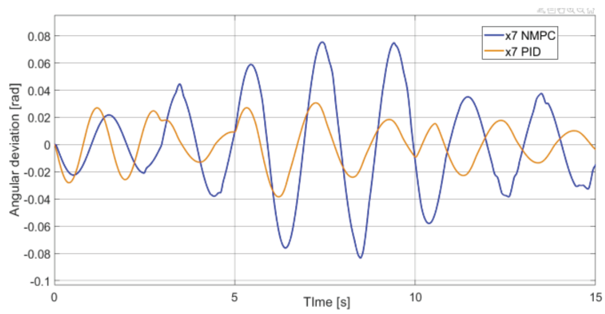

Figure 11. Obtained waveforms of x_7 control for both designed control systems

Even the highest checked value of this parameter does not allow this controller to fully cover the dynamics of the system related to the control of deviations x_5 and x_7 which would guarantee its full effectiveness. The other argument in favor of the PID control system is that it is less complex and can be easily implemented without involving huge time resources in the designing phase. Taking all these arguments into account, despite a very high potential of the predictive controller, its use for 3D crane control is not more advantageous than the PID control system.

5. Conclusion

The paper presents the process of designing the control system for a 3D crane. The mathematical model of the crane has been verified and the equivalent model of the Z-axis was proposed. Tuning the PID controllers and predictive controller are described, along with the implementation of both control systems and the comparative analysis of their performance. The synthesis process has turned out successful for both control systems as they provide correct realization of the reference trajectories while minimizing the load swing effect. Both solutions can be considered, however, the design and implementation of the PID structure control system is quicker and simpler than that of the predictive controller.

AUTHORS

Maciej Szafrański – Gdańsk University of Technology, Faculty of Electrical and Control Engineering, Poland, e-mail: szafmac@gmail.com.

Robert Piotrowski* – Gdańsk University of Technology, Faculty of Electrical and Control Engineering, Poland, e-mail: robert.piotrowski@pg.edu.pl.

*Corresponding author

References

[1] Q.T. Nguyen and V. Veselý, "Robust Decentralized PID Controller Design for the 3D Crane Process," M. Fikar and M. Kvasnica, eds., *Proceedings of the 18th International Conference on Process Control*, 2007, pp. 485–489.

[2] A. Cellmer, B. Banach, and R. Piotrowski, "Design of Modified PID Controllers for 3D Crane Control," *XIX National Conference on Automation* (KKA'2017), 18-21 Jun. 2017, (in:) W. Mitkowski et al., eds., *Trends in Advanced Intelligent Control, Optimization and Automation, Advances in Intelligent Systems and Computing*, vol. 577, Springer, pp. 77–86.

[3] P. Petrehus, Z. Lendek, and P. Raica, "Fuzzy Modeling and Design for a 3D Crane," Dept. Automation, Technical University of Cluj Napoca, 2013, Memorandumului 28, 400114.

[4] D. Antić, et al., "Anti-Swing Fuzzy Controller Applied in a 3D Crane System," *ETASR - Engineering, Technology & Applied Science Research*, vol. 2, no. 2, 2012, pp. 196–200.

[5] A. Aksjonov, V. Vodorozov, and E. Petlenkov, "Three-Dimensional Crane Modelling and Control Using Euler-Lagrange State-Space Approach and Anti-Swing Fuzzy Logic," *Electrical Control and Communication Engineering*, vol. 9, 2015, pp. 5–13.

[6] D. Schindele and H. Aschemann, "Fast Nonlinear MPC for an Overhead Travelling Crane," *Proceedings of the 18th World Congress The International Federation of Automatic Control,* 28 Aug. – 2 Sep 2011.

[7] A. Khalaf, et al., "Model-based Predictive Control of a Tower Crane," *MACE Technical Journal*, vol. 1, no. 1, Dec. 2019, pp. 25–31.

[8] N. Thi-Thuy Vu, et al., "Robust Adaptive Control of 3D Overhead Crane System. Adaptive Robust Control Systems," Mar. 2018.

[9] M. Pauluk, "Optimal and Robust Control of 3D crane," *Przegl¹d Elektrotechniczny,* vol. 92, no. 2, 2016.

[10] Y. Yoshida, "Feedback Control and Time-Optimal Control about Overhead Crane by Visual Servo and These Combination Control," *Intelligent Mechatronics*, G. Naik, ed., InTech, 2011.

[11] K.J. Aström and T. Hägglund, "PID Controllers: Theory, Design and Tuning. 2end Edition," *Instrument Society of America*, 1995.

[12] L. Grüne and J. Pannek, "Nonlinear Model Predictive Control. Theory and Algorithms. Second Edition," *Communications and Control Engineering*, Springer International Publishing Switzerland, 2011.